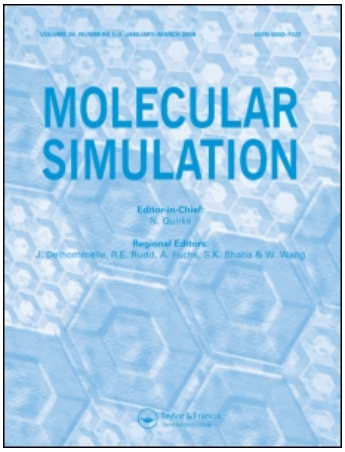

Molecular Simulation

Publication details, including instructions for authors and subscription information:
http://www.informaworld.com/smpp/title~content=t713644482

Adsorption of alkanes, alkenes and their mixtures in single-walled carbon nanotubes and bundles

S. Jakobtorweihen[a]; F. J. Keil[a]
[a] Institute of Chemical Reaction Engineering, Hamburg University of Technology, Hamburg, Germany

First published on: 21 September 2010

To cite this Article Jakobtorweihen, S. and Keil, F. J.(2009) 'Adsorption of alkanes, alkenes and their mixtures in single-walled carbon nanotubes and bundles', Molecular Simulation, 35: 1, 90 — 99, First published on: 21 September 2010 (iFirst)
To link to this Article: DOI: 10.1080/08927020802378936
URL: http://dx.doi.org/10.1080/08927020802378936

Molecular Simulation
Vol. 35, Nos. 1–2, January–February 2009, 90–99

Taylor & Francis
Taylor & Francis Group

Adsorption of alkanes, alkenes and their mixtures in single-walled carbon nanotubes and bundles

S. Jakobtorweihen and F.J. Keil*

Institute of Chemical Reaction Engineering, Hamburg University of Technology, Hamburg, Germany

(*Received 24 April 2008; final version received 30 July 2008*)

Monte Carlo simulations are employed to calculate pure component adsorption isotherms of linear alkanes (C2–C12), alkenes (C2–C4) and some of their binary mixtures (ethane–ethene, propane–propene, *cis*-2-butene–*trans*-2-butene, propene-1-butene) in single-walled carbon nanotubes. The zigzag structures of carbon nanotubes (CNTs) of various diameters [(10,0), (20,0), (30,0) and (40,0)] are used. Furthermore, Henry coefficients and isosteric heats of adsorption are calculated. The dependence of these properties as a function of chain length (carbon number) is presented. The relation of the critical parameters and the isosteric heats of adsorption, observed earlier for zeolites, could be confirmed for CNTs. The adsorption behaviour of 1-butene, *cis*-2-butene and *trans*-2-butene are compared in detail. Radial density profiles of 1-butene in a (40,0) nanotube for various pressures reveal a build-up of three layers inside the pores with increasing pressure. For all investigated binary mixtures, one of the component isotherms shows a distinct maximum owing to an entropic effect and non-idealities of the bulk gas phase behaviour. Additionally, adsorption in CNT bundles in hexagonal arrangement is studied. Depending on the pore arrangements, pore diameters and pressures, a fraction of the adsorbed gases is located in the interstitial space.

Keywords: carbon nanotube; adsorption; alkanes; alkenes; molecular simulations

1. Introduction

After the discovery of carbon nanotubes (CNTs) by Iijima [1], these materials were considered for adsorption of various gases. Besides hydrocarbons [2–6], adsorption of other molecules and mixtures on single-walled CNTs (SWCNTs) were investigated, like hydrogen [7–9], nitrogen [10–13], nitrogen/oxygen [14,15], water [16], neon [17], helium [18] and xenon [19]. Cao et al. [3] investigated the adsorption of methane on triangular arrays of SWCNTs at room temperature with the grand canonical Monte Carlo (GCMC) method. The carbon atoms on the tubular wall were structured according to the armchair arrangement and the 'site-to-site method' was used to calculate the interaction between a methane molecule inside the tube and a carbon atom on the tubular wall. The gap between the tubes was varied in order to find the optimum gap with respect to the amount of adsorbed methane. Jiang et al. [4] studied adsorption and separation of linear (C1–C5) and branched (C5 isomers) alkanes on (10,10) SWCNT bundles at 300 K using configurational-bias Monte Carlo (CBMC) simulations. For pure linear alkanes, the limiting adsorption properties at zero coverage exhibit a linear relation with the alkane carbon number; long alkanes are more adsorbed at low pressures, but the reverse is found for short alkanes at high pressures. For pure branched alkanes, the linear isomer adsorbs to a greater extent than its branched counterparts. For a five-component mixture of C1–C5 linear alkanes, the long alkane adsorption first increases and then decreases with increasing pressure, but the short alkane adsorption is continuously increasing and progressively replaces the long alkanes at high pressures due to the size entropy effect. This phenomenon was already detected before in [20,21] for silicalite and by Heyden et al. [22] for binary mixtures of methane, ethane, propane and tetrafluormethane in SWCNTs by using CBMC simulations. At high loadings, a maximum occurs with increasing pressure in the absolute adsorption isotherm of one or both adsorbing species. It was detected that there exist two fundamentally different reasons for this maximum. First, the size entropy effect [23] and second, non-ideality effects of the gas phase [22] can be made responsible for this maximum. If owing to non-ideality effects of the gas phase, the fugacity of one component does not increase as steeply with pressure as the other component, a maximum can occur in the absolute adsorption isotherm of this component [22]. It must be stressed that the displaced component is not necessarily the larger molecule. Similar effects were also observed by Jakobtorweihen et al. [24] for adsorption of alkenes in various zeolites.

Kondratyuk et al. [5] found three well-defined adsorption sites on opened SWCNTs (tube diameter 13.6 Å) by temperature programmed desorption measurements for several alkanes. On the basis of hybrid Monte Carlo simulations, the two highest binding energy adsorption sites correspond to adsorption inside tubes

*Corresponding author. Email: keil@tu-harburg.de

ISSN 0892-7022 print/ISSN 1029-0435 online

DOI: 10.1080/08927020802378936
http://www.informaworld.com

and to groove sites between adjacent nanotubes in bundles. The third highest binding energy corresponds to sites on the exterior nanotube surface. Burde et al. [2] investigated the kinetics of gas uptake on different regions of CNT bundles by means of the kinetic Monte Carlo scheme. On both external and internal sites of a nanotube bundle, equilibration times are observed to decrease linearly as the coverage increases toward monolayer completion; the rate at which this occurs strongly depends on the ratio between the binding energy and the temperature. For low coverages, very long equilibration times can be observed. The adsorption in pore-like phases is typically two orders of magnitude slower than that of external phases.

A survey of computational techniques for CNTs was presented by Rafii-Tabar [25].

The motivation of this paper is the investigation of alkene adsorption in SWCNTs and the separation potential of linear alkanes and alkenes in CNTs. Furthermore, the effect of pore diameters on adsorption and the adsorption in the interstitial space in CNT-bundles is evaluated. Hysteresis is not investigated in this work. Jiang et al. [6] have found hysteresis for alkane adsorption inside a CNT having a larger diameter as the widest pore employed in this study, but the dependence of hysteresis on tube size was not studied.

The outline of this article is as follows: in the next section, the models underlying our simulations are explained and details of the simulations are given. In Section 3, the results are shown and discussed. We end with a conclusion in the last section.

2. Simulation details

Intermolecular interactions were modelled with the truncated Lennard-Jones (LJ) 12–6 potential. The fluid molecules were modelled as united-atoms. For the intramolecular and the fluid–fluid intermolecular interactions, the TraPPE force field was used [26,27], where the bond angle bending is described by a harmonic potential and the bond torsion with a 3-cosine-fourier potential. For *trans*- and *cis*-2-butene, an harmonic torsional potential is used. In the TraPPE force field, the bond lengths are fixed. To check the influence of this assumption, some systems were re-simulated with an harmonic bond potential, but we found no influence on the adsorption isotherms. The carbon LJ parameters were taken from [28]. Lorentz–Berthelot mixing rules were used to determine the interactions of unlike molecular centres. The LJ parameters are listed in Table 1. For the LJ interactions, a cutoff radius of 14 Å was used in combination with the usual tail corrections [29]. Note that Macedonia and Maginn [30] have shown that tail corrections do not apply to adsorption in nanoporous materials as tail corrections assume a homogenous distribution of the molecules behind the cutoff. As the TraPPE force field includes tail corrections and to date no force field that was explicitly developed for hydrocarbon–CNT interactions is available (lack of experimental data prevents developing such parameters), tail corrections were used in this study. Moreover, Macedonia and Maginn [30] have shown that the influence of tail correction on calculated adsorption isotherms for butane in silicalite is small. The influence on the systems studied in this work is also minor. For example, ethane at a temperature of 300 K and a pressure of 1 bar inside a (20,0) CNT shows an adsorption capacity of 3.69 mol/kg. This value reduces to 3.34 mol/kg when tail corrections are not used.

Table 1. LJ parameters and their source.

Centre	σ (Å)	ε/k_B (K)	Ref.
CH_4	3.73	148	[26]
CH_3 (sp^3)	3.75	98	[26]
CH_2 (sp^3)	3.95	46	[26]
CH_2 (sp^2)	3.675	85	[27]
CH (sp^2)	3.73	47	[27]
Carbon	3.4	28	[28]

The size and helicity of CNTs is specified by two integer numbers [31] n_1 and n_2, so they can be unambiguously labelled as (n_1,n_2). All results in this work were obtained with SWCNTs in a zigzag structure. For $n_2 = 0$, tubes have the zigzag structure, at which one carbon–carbon bond is parallel to the pore axis. The investigated tubes have the following diameters (defined by the position of the carbon nuclei): 7.8 Å (10,0), 15.7 Å (20,0), 23.5 Å (30,0) and 31.3 Å (40,0). Note that although deformations can occur especially for larger tubes, we have simulated all nanotubes as 'perfect' SWCNTs. As framework flexibility has a vanishing influence on adsorption isotherms [32], we modelled the nanotubes as rigid (carbon atoms fixed on their positions). Note that CNT flexibility can have a dramatic influence on the dynamics of guest molecules [33]. The rigid framework assumption allows the use of interpolation grids for the calculation of the fluid-nanotube interactions. A grid fineness of 0.065 Å was used. The nanotubes length was set to 102 Å. However, effectively an infinitely long tube was simulated as usual periodic boundaries [34] were used for the direction parallel to the pore axis.

GCMC simulations were performed to calculate adsorption isotherms. In the grand canonical ensemble, the number of particles can fluctuate, whereas the chemical potentials, the temperature and the volume are constant. For details about the GCMC method, see [29]. For effective simulations of molecules, the configurational bias Monte Carlo method was used, which allows the growth of a molecule atom by atom [35,36]. The following Monte Carlo trials were performed during a GCMC simulations: displacement of a molecule, rotation of a molecule around its centre of mass, partial and total

regrowth of a molecule, and molecule exchange with a reservoir. Additionally, for simulating mixtures particle identity changes were carried out. All acceptance rules are summarised in an earlier publication [37]. The number of generated configurations depends on the system. For all studied systems more than 1.5 million Monte Carlo trials were performed for equilibration and more than 8 million trials were carried out for sampling. For the molecule exchange acceptance rules either the bulk chemical potentials or the bulk fugacities must be specified [37]. The fugacities were calculated with the Peng–Robinson equation of state using parameters taken from [38]. To determine the Henry coefficients and the isosteric heats of adsorption Monte Carlo simulations in the canonical ensemble in combination with the CBMC technique were carried out for the zero loading limit [39] (only one fluid molecule). Additionally, a separate simulation in the ideal gas state was necessary. The Henry coefficient can then be calculated as

$$K_{\mathrm{H}} = \beta \frac{\langle \mathcal{W} \rangle}{\langle \mathcal{W}_{\mathrm{IG}} \rangle}, \tag{1}$$

where $\beta = 1/(k_{\mathrm{B}}T)$ and $\mathcal{W}$ is the normalised Rosenbluth factor calculated according to the CBMC approach [29,35,36]. The subscript IG is used to indicate the ideal gas state. The angular brackets denote ensemble averages. The term k_{B} is the Boltzmann constant and T the temperature. The isosteric heat of adsorption has been calculated from

$$q_{\mathrm{st}}^{0} = \langle U \rangle_{\mathrm{IG}} - \langle U \rangle + k_{\mathrm{B}}T, \tag{2}$$

where U is the total energy.

3. Results and discussion

The first results in this section are for adsorption inside single CNTs; thereafter results for CNT bundles are shown. All presented isotherms are absolute adsorption isotherms. The pure component adsorption isotherms are presented by plotting the amount of moles adsorbed per unit weight of adsorbent as a function of pressure. Error bars have not been included in the figures since they are, in almost all cases, smaller than the symbols. In Figures 1 and 2, the pure component adsorption isotherms of ethane, ethene, propane and propene for various SWCNTs at 300 K are presented.

As can be seen from Figure 1, at low pressures more alkane molecules are adsorbed than alkenes and the adsorption in narrow pores is stronger than in wider pores. The interaction of the adsorbed molecules is stronger in narrow pores and the isotherms level off at lower pressures than in larger pores. As expected, at higher pressures more molecules can be adsorbed inside the larger pores.

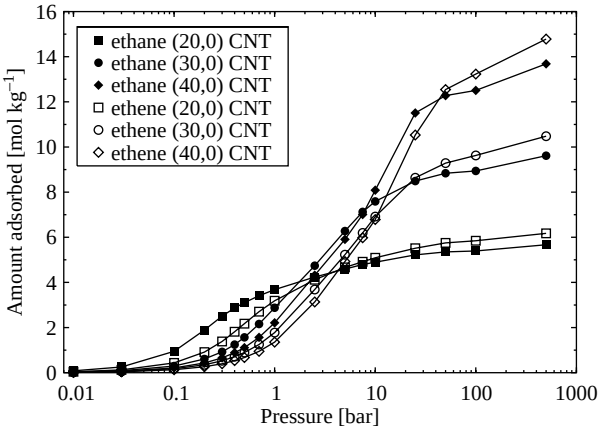

Figure 1. Adsorption isotherms of ethane and ethene in different CNTs at 300 K. Lines are added to guide the eye.

A comparison between Figures 1 and 2 shows that at low pressures more propane molecules are adsorbed than ethane, but at high pressure the number of adsorbed ethane molecules is higher as the required space is smaller than for propane. At low pressures, both ethene and propene are adsorbed in a smaller amount than the respective alkanes, and at high pressures, it is the opposite. This is caused by the larger number of interaction sites of alkanes. At high pressure, the smaller size of alkenes is decisive.

In Figure 3, the adsorption isotherms of 1-butene, *cis*-butene and *trans*-butene at 300 K in (20,0) and (40,0) SWCNTs are presented. As before, at low pressures more molecules in the narrow pores are adsorbed and at high pressure it is opposite. The adsorption behaviour of the three alkenes is quite similar.

The development of adsorption layers for 1-butene is shown in detail in Figure 4. Radial density (RD) profiles of 1-butene inside a (40,0) SWCNT at 300 K and four pressures (0.1, 0.4, 0.6 and 100 bar) are presented. Additionally, the

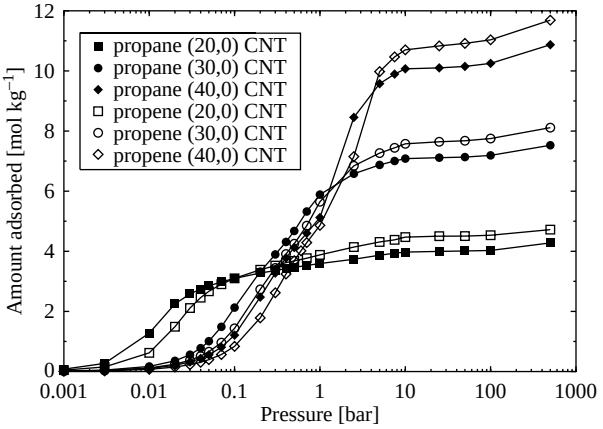

Figure 2. Adsorption isotherms of propane and propene in different CNTs at 300 K. Lines are added to guide the eye.

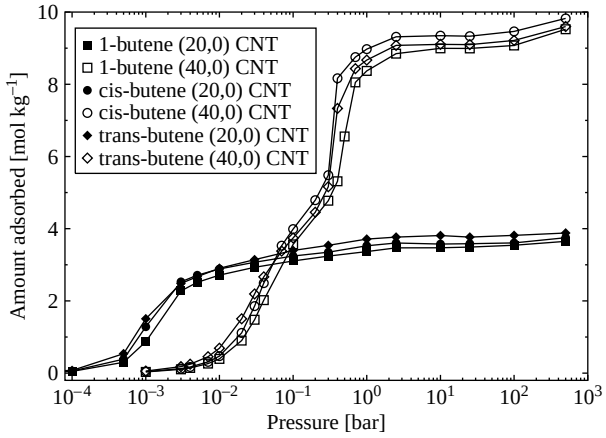

Figure 3. Adsorption isotherms of 1-butene, *cis*-2-butene and *trans*-2-butene in different CNTs at 300 K. Lines are added to guide the eye.

adsorption isotherm is given, where the state point for which the RD profile is shown is marked with a cross. At 0.1 bar, the first adsorption layer at a distance of 0.4 nm from the wall is formed. At a slightly higher pressure of 0.4 bar, the formation of a second layer is initiated. The centre part of the tube (1.2–1.6 nm) is still empty. This changes at 0.6 bar where the third layer is slowly built up and the second layer gets more distinctive. Eventually, at 100 bar the third layer is formed and the centre part of the tube is filled.

Figure 5 shows the calculated Henry coefficients of *n*-alkanes as a function of their carbon numbers at 300 K in SWCNTs of various diameters. These simulations were executed for the zero loading limit. The very strong interaction between the (10,0) CNT and the alkanes is demonstrated by the rather large Henry coefficients compared to the values for the wider tubes. The alkenes (Figure 6) show a similar behaviour. A comparison of the Henry coefficients of 1-butene, *cis*-2-butene and *trans*-2-butene in (10,0) carbon tubes reveals that *trans*-2-butene adsorbs strongest and the comparatively bulky *cis*-2-butene adsorbs weakest.

For both alkanes and alkenes, the differences between the Henry coefficients become smaller, the larger the tube diameters are. This is also supported by the isosteric heats of adsorption in Figures 7 and 8. The heats of adsorption show a linear dependence on the chain length for alkanes and alkenes. Note that both the chain length dependency

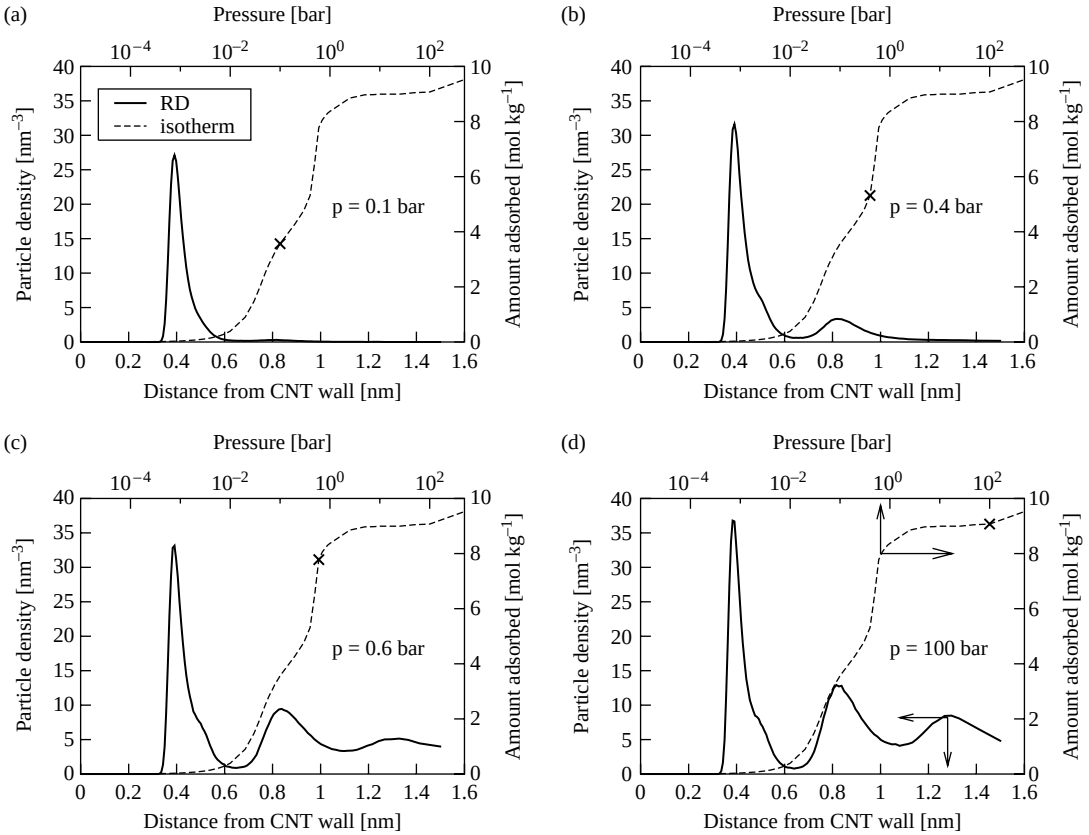

Figure 4. Radial density (RD) profiles represent 1-butene distributions inside a (40,0) CNT at 300 K. The adsorption isotherm of 1-butene at 300 K is plotted on the secondary axes, the state point for which the RD profile is shown is marked with a cross. RD profiles for four different pressures are shown: (a) 0.1 bar, (b) 0.4 bar, (c) 0.6 bar and (d) 100 bar.

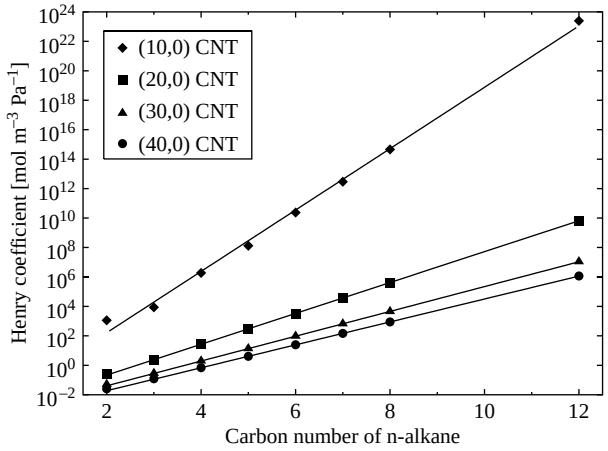

Figure 5. Henry coefficients of *n*-alkanes as functions of their carbon numbers at 300 K in different CNTs. Lines represent exponential fits.

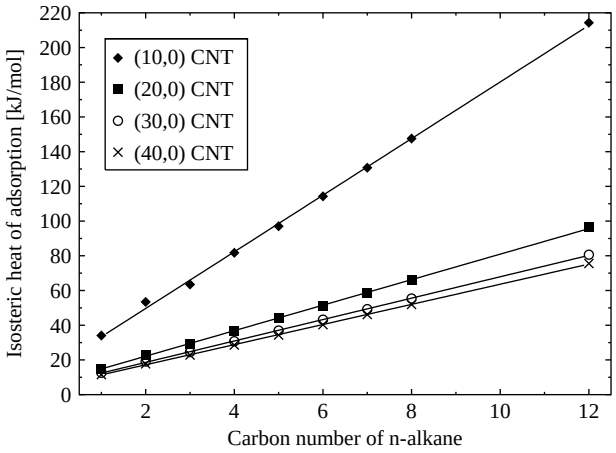

Figure 7. Isosteric heats of adsorption of *n*-alkanes as function of their carbon numbers for the zero loading limit at 300 K in different CNTs. Lines represent linear fits.

of the Henry coefficients and the chain length dependency of the heats of adsorption were also observed experimentally for alkanes in zeolites [40]. Furthermore, these dependencies were already observed with molecular simulation methods for the adsorption of alkanes in CNT bundles [4] and in agreement with experiments, for the adsorption in silicalite [20,41].

In Table 2, a comparison of Henry coefficients, K_H and isosteric heats of adsorption, q_{st}, for the butenes inside CNTs of different sizes is presented. Unlike the (10,0) tube (Figures 6 and 8), the larger nanotubes show the following sequence in the K_H and q_{st} values: 1-butene $<$ *cis*-2-butene $<$ *trans*-2-butene. In the (10,0) nanotube the order is *cis*-2-butene $<$ 1-butene $<$ *trans*-2-butene. In the narrow (10,0) tube, the structure of the 1-butene molecule is changed compared to the structure in the ideal gas state, whereas the structure of 1-butene in the wider tubes is similar to the structure in the ideal gas state. The structure of 1-butene in a (10,0) CNT is closer to *trans*-2-butene than in the other tubes. Moreover, in the (10,0) nanotube 1-butene is never in the *cis* state, whereas in the ideal gas state a small fraction of 1-butene molecules can be found in the *cis* configuration. Thus, the 1-butene molecule structure is adjusted to better fit these molecules into the narrow channels.

For silicalite-1 and highly de-aluminated Y zeolite (US-Ex), Thamm et al. [42] found a linear relation between the experimental initial heats of adsorption of *n*-alkanes and cyclohexane and their critical parameters

$$q_{st}^{0} = D\frac{T_C}{p_C^{0.5}}, \tag{3}$$

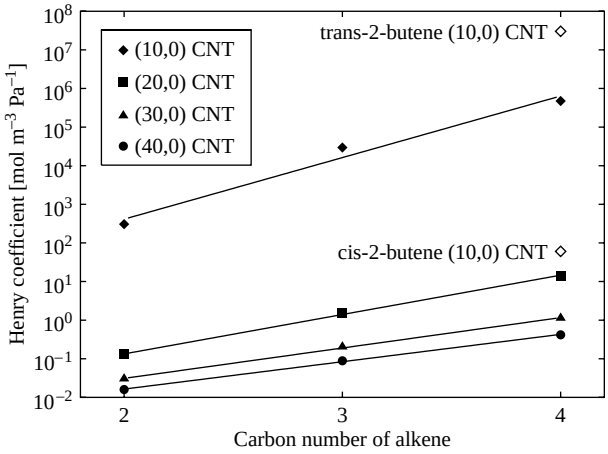

Figure 6. Henry coefficients of 1-alkenes as functions of their carbon numbers at 300 K in different CNTs. Lines represent exponential fits. Additionally, the results for *cis*-2-butene and *trans*-2-butene in the (10,0) CNT are shown (open symbols).

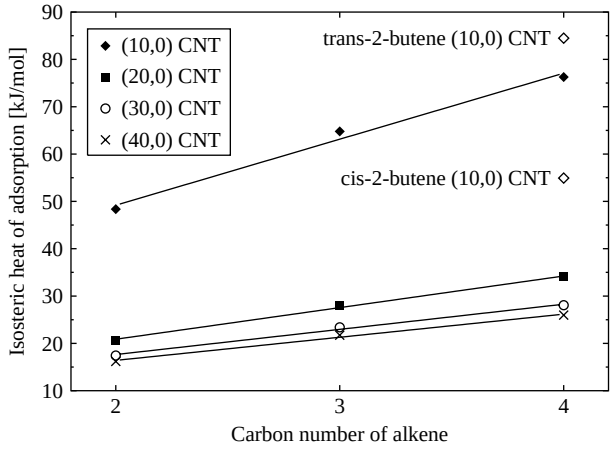

Figure 8. Isosteric heats of adsorption of 1-alkenes as function of their carbon numbers for the zero loading limit at 300 K in different CNTs. Lines represent linear fits. Additionally, the results for *cis*-2-butene and *trans*-2-butene in the (10,0) CNT are shown (open symbols).

Table 2. Comparison of the Henry coefficients, K_H and the isosteric heats of adsorption, q_{st}, for the butenes in different CNTs.

Species	CNT	K_H (mol m^3 Pa^{-1})	q_{st} (kJ mol^{-1})
1-Butene	(10,0)	$4.733 \times 10^5_{0.158}$	$76.26_{0.04}$
cis-2-Butene	(10,0)	$6.047 \times 10^1_{0.603}$	$54.92_{0.10}$
trans-2-Butene	(10,0)	$3.938 \times 10^7_{0.071}$	$85.62_{0.03}$
1-Butene	(20,0)	$14.214_{0.027}$	$34.04_{0.01}$
cis-2-Butene	(20,0)	$16.694_{0.051}$	$35.37_{0.01}$
trans-2-Butene	(20,0)	$22.092_{0.055}$	$36.36_{0.02}$
1-Butene	(30,0)	$1.127_{0.002}$	$28.07_{0.01}$
cis-2-Butene	(30,0)	$1.319_{0.004}$	$29.48_{0.02}$
trans-2-Butene	(30,0)	$1.879_{0.006}$	$30.72_{0.01}$
1-Butene	(40,0)	$0.417_{0.001}$	$25.97_{0.01}$
cis-2-Butene	(40,0)	$0.486_{0.001}$	$27.34_{0.02}$
trans-2-Butene	(40,0)	$0.691_{0.002}$	$28.64_{0.02}$

All results correspond to a temperature of 300 K. Errors are given in the subscripts.

where D represents the proportional constant. These authors showed that the isosteric heat of adsorption of ethene and 1-butene is also determined by this relation. Jakobtorweihen et al. [24] confirmed these findings by simulations of a broad variety of alkanes and alkenes in silicalite-1. Bruce et al. [43] found this result also for graphitized black powders. In Figure 9, the relation given in Equation 3 is confirmed for alkanes and some alkenes in SWCNTs of various diameters. Only the bulky *cis*-2-butene shows a somewhat larger deviation in the very narrow (10,0) tube.

In Figure 10(a), simulated adsorption isotherms of the binary mixture of ethane and ethene inside a (20,0) CNT at 300 K for a fixed equimolar bulk phase composition are presented. Additionally, the selectivity is shown. The selectivity of component 1 with respect to component

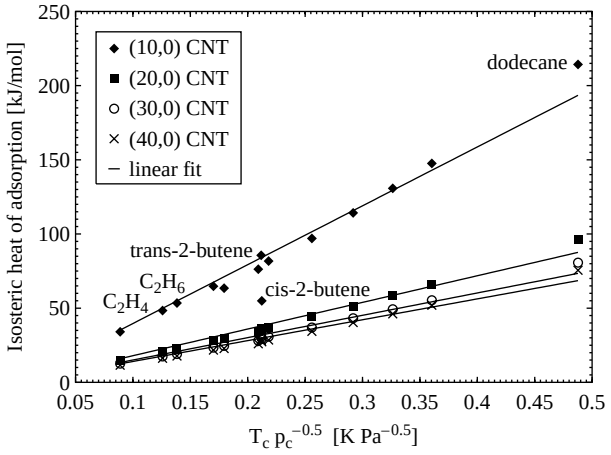

Figure 9. Dependence of the simulated isosteric heats of adsorption for the zero loading limit at 300 K in different CNTs on the critical data for hydrocarbons. Lines represent linear fits, where the fit constants are: $D_{10} = 396.64$, $D_{20} = 179.66$, $D_{30} = 150.66$ and $D_{40} = 140.66$.

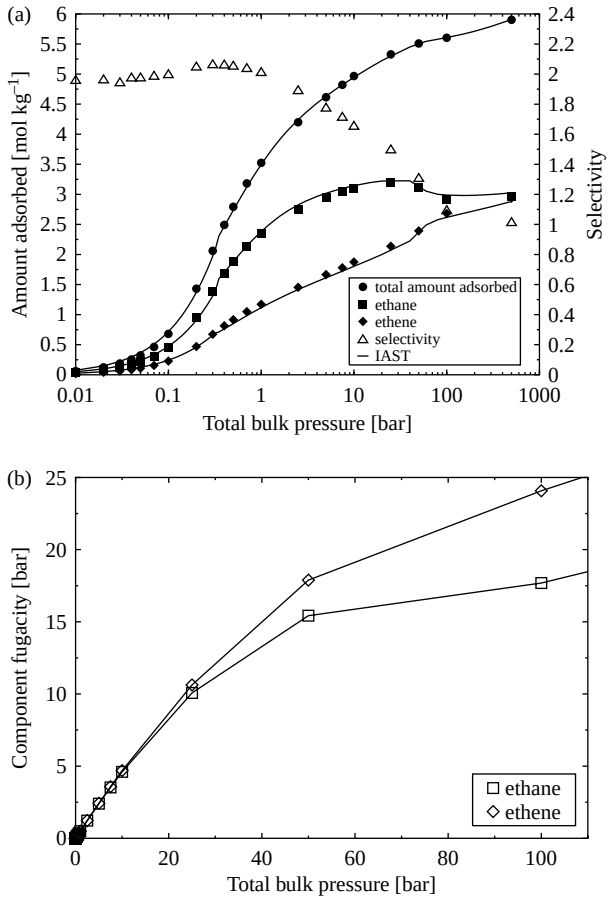

Figure 10. (a) Simulated adsorption isotherm of a binary mixture of ethane and ethene inside a (20,0) CNT for a fixed equimolar bulk phase composition at 300 K and selectivity of ethane with respect to ethene. Lines represent results of the IAST. (b) The corresponding component fugacities, calculated with the Peng–Robinson equation of state, are plotted against total bulk pressure. Lines are added to guide the eye.

2 is defined as

$$S_{12} = \frac{x_1/y_1}{x_2/y_2}, \tag{4}$$

where x and y are the mole fractions of the adsorbed phase and the bulk phase, respectively. The lines represent results obtained by the ideal adsorption solution theory (IAST) [44]. For these calculations the pure component adsorption isotherms detailed in this work were used. To take into account, the non-ideality of the gas phase, we have used the fugacities rather than the pressure for calculating the IAST isotherms. Like for the pure component adsorption, at low pressure more ethane than ethene is adsorbed. At high pressures the entropic effect [23] leads to a reversal. Thus, we observe a distinct maximum in the ethane isotherm, which is also calculated by the IAST. A further reason for the maximum of the isotherms is a non-ideality effect of the gas phase. Details

are given by Heyden et al. [22]. In Figure 10(b), the component fugacities of ethane and ethene in the gas phase as calculated by the Peng–Robinson equation of state show a difference between the fugacities from about 25 bar on. Close to this value is the maximum of the adsorption isotherm of ethane. These maxima were also observed by Jiang et al. [4], Heyden et al. [22] for CNTs and by Jakobtorweihen et al. [24] for zeolites, among others. Note that Jiang et al. [4] have also observed distinct maxima in the selectivities for mixtures of C5 isomers. The selectivity drops from about two at low pressures to about one at high pressures.

A qualitatively similar behaviour can be observed in Figure 11 for a propane and propene binary mixture. The selectivities for this mixture are closer to one. The larger the hydrocarbons the weaker the influence of the double bond. Hence, the higher the carbon number the higher the similarity of an alkane and 1-alkene having

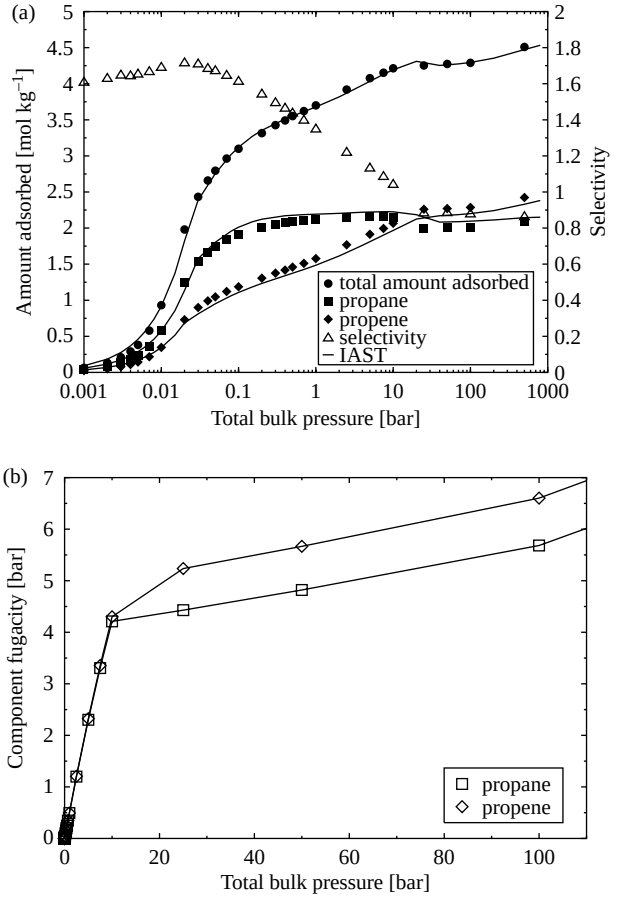

Figure 11. (a) Simulated adsorption isotherm of a binary mixture of propane and propene inside a (20,0) CNT for a fixed equimolar bulk phase composition at 300 K and selectivity of propane with respect to propene. Lines represent results of the IAST. (b) The corresponding component fugacities, calculated with the Peng–Robinson equation of state, are plotted against total bulk pressure. Lines are added to guide the eye.

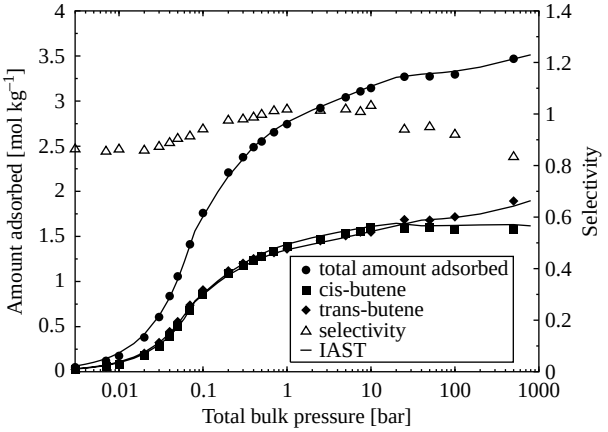

Figure 12. Simulated adsorption isotherm of a binary mixture of *cis*-butene and *trans*-butene inside a (20,0) CNT for a fixed equimolar bulk phase composition at 400 K and selectivity of *cis*-butene with respect to *trans*-butene. Lines represent results of the IAST.

the same carbon number. It can be concluded that for these kind of alkane–alkene mixtures, the separation is more difficult the higher the carbon number.

Figure 12 shows the adsorption isotherms of *cis*-2-butene and *trans*-2-butene inside a (20,0) SWCNT at 400 K for a fixed equimolar bulk phase composition. The lines present again the IAST results. Initially, the adsorption isotherms are very similar. At very high pressures, a configurational entropic effect occurs and the isotherms start to diverge. An effective separation of these isomers is therefore, if at all, only possible at very high pressures. A better separation can be achieved for a binary mixture of propane and 1-butene (see Figure 13).

All results presented above dealt with adsorption inside and only inside, a single CNT. In order to investigate the

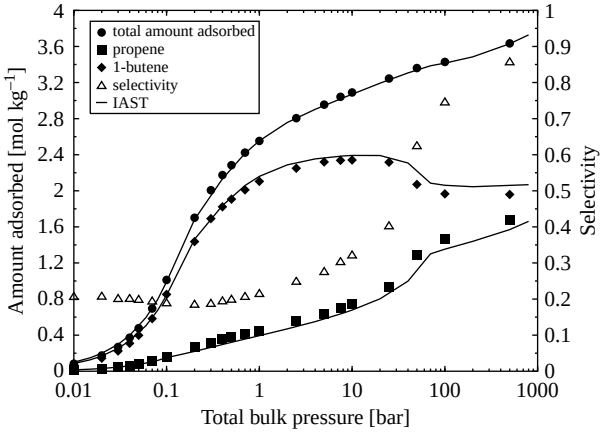

Figure 13. Simulated adsorption isotherm of a binary mixture of propene and 1-butene inside a (20,0) CNT for a fixed equimolar bulk phase composition at 400 K and selectivity of propene with respect to 1-butene. Lines represent results of the IAST.

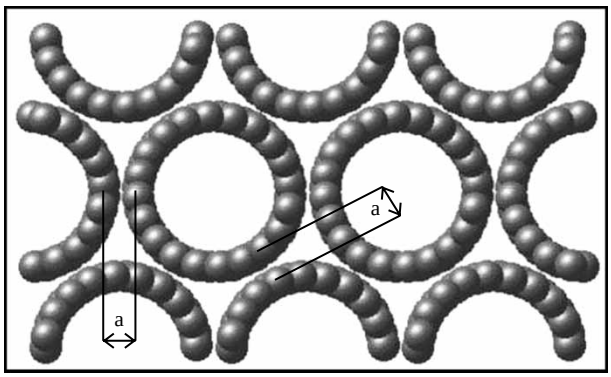

Figure 14. CNTs in a hexagonally arranged bundle. The $x-y$ plan of the bundle of (20,0) nanotubes are shown as it was used in the simulations. For all investigated bundles a was set to 0.36 nm.

adsorption in the interstitial space of bundles of SWCNTs, hexagonally arranged bundles of SWCNTs with various diameters were investigated. The distance a (see Figure 14) was set to 0.36 nm. In Figure 15, the fraction of ethane molecules located in the interstitial space of different SWCNT bundles at 300 K is shown.

As the interstitial space is small, no ethane molecules adsorb in the interstitial space of (10,0) tubes in a hexagonal arrangement. Inside (20,0) tubes, the interstitial space is just large enough to adsorb ethane molecules (see Figure 16), but a pressure of at least 1 bar is necessary to initiate a measurable adsorption (Figure 15).

For the (30,0) and (40,0) tubes in hexagonal arrangement, ethane molecules at low pressure preferentially adsorb in the interstitial space. Due to the wall surrounding this is the energetically most favourable position (see also Figure 16). From about 0.01 bar on the

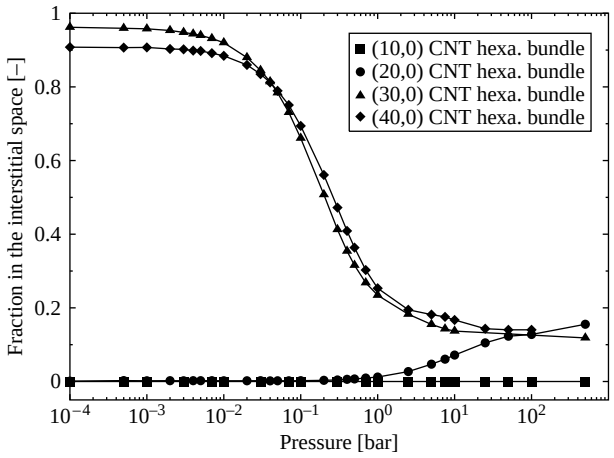

Figure 15. Fraction of ethane located in the interstitial space of a hexagonally arranged CNT bundle at a temperature of 300 K. All bundles contain only one type of nanotubes. Lines are added to guide the eye.

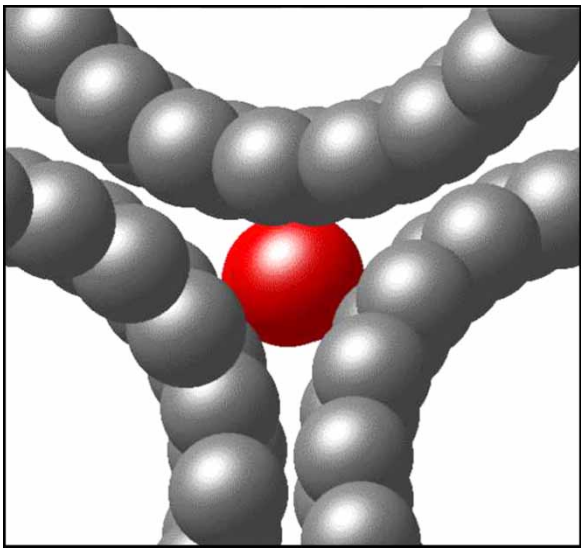

Figure 16. The snapshot displays an ethane molecule in the interstitial space of a hexagonal arranged bundle of (20,0) CNTs.

interstitial space for (30,0) and (40,0) tubes in hexagonal arrangement are nearly filled, and adsorption inside the tubes starts (see Figure 15).

In this study, the distance of the tubes $a = 0.36$ nm (see Figure 14) was chosen according to the employed force field parameters ($\sigma_C = 0.34$ nm and the position of the minimum $2^{1/6}\sigma_C = 0.38$ nm). Note that in other studies [45], the tube–tube distance is revealed to be smaller than 0.36 nm. Whether or not ethane adsorbs in the interstitial space is strongly dependent on the tube–tube distances and the nanotube radii. However, the recently produced CNT-membranes contain CNTs encapsulated in a matrix [46,47], so that the interstitial space is not accessible for adsorption. Note that for a comparison between measured adsorption isotherms and simulations the real tube diameters and tube arrangements are needed. Furthermore, the tubes have to be open at both ends which was obviously not always the case in previous measurements [48].

4. Conclusion

Molecular simulations have been performed to evaluate the adsorption isotherms of alkanes, alkenes and some of their binary mixtures. As expected, at low pressures, the adsorption in narrow pores is stronger than in wider pores and more alkanes than alkenes are adsorbed under these conditions. At higher pressures, more molecules inside larger pores can be adsorbed. At low pressures, more alkanes are adsorbed than the corresponding alkenes, at high pressures it is the opposite. Short and long alkanes show, in principle, the same adsorption isotherm shapes. The adsorption isotherms of 1-butene, *cis*-2-butene and

trans-2-butene are quite similar. The Henry coefficients and isosteric heats of adsorption of all alkanes and alkenes investigated revealed a very strong interaction with the (10,0) CNT ($d_{CNT} = 7.8$ Å). For both alkanes and alkenes the differences between the Henry coefficients and isosteric heats of adsorption become smaller, the larger the tube diameters are. The relation between critical parameters and the isosteric heats of adsorption by Thamm et al. [42] could be confirmed for adsorption in CNTs. For each of the binary mixtures, one component isotherm shows a distinct maximum. This could be attributed to a configurational entropy effect inside the pores and non-idealities in the bulk phase. The IAST calculations also showed these maxima and coincided with the simulation results. The selectivity of the ethane–ethene mixture is higher at low pressures than for propane–propene. *Cis*- and *trans*-2-butene can only be separated, if at all, at very high pressures. The larger the difference in the carbon numbers of the co-adsorbing species the larger the selectivity. The selectivities are low when both components (*n*-alkane and 1-alkene) have the same number of carbons. At low pressures, a considerable amount of ethane is adsorbed in the interstitial space of the here investigated hexagonal arrangements (tube–tube distance $a = 0.36$ nm) of (30,0) and (40,0) CNTs.

Acknowledgements

This work was supported by the Deutsche Forschungsgemeinschaft (DFG) in priority program SPP 1155. We thank Niels Hansen for help with IAST calculations.

References

[1] S. Iijima, *Helical microtubules of graphitic carbon*, Nature 354 (1991), pp. 56–58.
[2] J.T. Burde and M.M. Calbi, *Physisorption kinetics in carbon nanotube bundles*, J. Phys. Chem. C 111 (2007), pp. 5057–5063.
[3] D. Cao, X. Zhang, J. Chen, W. Wang, and J. Yun, *Optimization of single-walled carbon nanotube arrays for methane storage at room temperature*, J. Phys. Chem. B 107 (2003), pp. 13286–13292.
[4] J. Jiang, S.I. Sandler, M. Schenk, and B. Smit, *Adsorption and separation of linear and branched alkanes on carbon nanotube bundles from configurational-bias Monte Carlo simulation*, Phys. Rev. B 72 (2005), 045447.
[5] P. Kondratyuk, Y. Wang, J.K. Johnson, and J.T. Yates, *Observation of a one-dimensional adsorption site on carbon nanotubes: Adsorption of alkanes of different molecular lengths*, J. Phys. Chem. B 109 (2005), pp. 20999–21005.
[6] J. Jiang, S.I. Sandler, and B. Smit, *Capillary phase transitions of* n-*alkanes in a carbon nanotube*, Nano Lett. 4 (2004), pp. 241–244.
[7] F. Darkim, P. Melbrunot, and G.P. Tartaglia, *Review of hydrogen storage by adsorption in carbon nanotubes*, Int. J. Hydrogen Energy 27 (2002), pp. 193–202.
[8] V. Meregalli and M. Parinello, *Review of theoretical calculations of hydrogen storage in carbon-based materials*, Appl. Phys. A 72 (2001), pp. 143–146.
[9] G. Froudakis, *Hydrogen interaction with carbon nanotubes: A review of* ab initio *studies*, J. Phys. Condens. Matter 14 (2002), pp. R453–R465.
[10] J.I. Paredes, F. Suárez-García, S. Villar-Rodil, A. Martínez-Alonso, J.M.D. Tascón, and E.J. Bottani, *n2 physisorption on carbon nanotubes: Computer simulation and experimental results*, J. Phys. Chem. B 107 (2003), pp. 8905–8916.
[11] J. Jiang and S.I. Sandler, *Nitrogen adsorption on carbon nanotube bundles: Role of the external surface*, Phys. Rev. B 68 (2003), 245412.
[12] J. Jiang, N.J. Wagner, and S.I. Sandler, *A Monte Carlo simulation study of the effect of carbon topology on nitrogen adsorption on graphite, a nanotube bundle, C_{60} fullerite, C_{168} schwarzite, and a nanoporous carbon*, Chem. Chem. Phys. 6 (2004), pp. 4440–4444.
[13] G. Arora, N.J. Wagner, and S.I. Sandler, *Adsorption and diffusion of molecular nitrogen in single wall carbon nanotubes*, Langmuir 20 (2004), pp. 6268–6277.
[14] J. Jiang and S.I. Sandler, *Nitrogen and oxygen mixture adsorption on carbon nanotube bundles from molecular simulation*, Langmuir 20 (2004), pp. 10910–10918.
[15] G. Arora and S.I. Sandler, *Air separation by single wall carbon nanotubes: Thermodynamics and adsorptive selectivity*, J. Chem. Phys. 123 (2005), 044705.
[16] A. Striolo, A.A. Chialvo, K.E. Gubbins, and T. Cummings, *Water in carbon nanotubes: Adsorption isotherms and thermodynamic properties from molecular simulation*, J. Chem. Phys. 122 (2005), 234712.
[17] M.C. Gordillo, L. Brualla, and S. Fantoni, *Neon adsorbed in carbon nanotube bundles*, Phys. Rev. B 70 (2004), 245420.
[18] B. Marcone, E. Orlandini, F. Toigo, and F. Ancilotto, *Condensation of helium in interstitial sites of carbon nanotubes bundles*, Phys. Rev. B 74 (2006), 085415.
[19] V.V. Simonyan, J.K. Johnson, A. Kuznetsova, and J.T. Yates, *Molecular simulation of xenon adsorption on single-walled carbon nanotubes*, J. Chem. Phys. 114 (2001), pp. 4180–4185.
[20] T.J.H. Vlugt, R. Krishna, and B. Smit, *Molecular simulations of adsorption isotherms for linear and branched alkanes and their mixtures in silicalite*, J. Phys. Chem. B 103 (1999), pp. 1102–1118.
[21] Z. Du, G. Manos, T.J.H. Vlugt, and B. Smit, *Molecular simulation of adsorption of short linear alkanes and their mixtures in silicalite*, AIChE J. 44 (1998), pp. 1756–1764.
[22] A. Heyden, T. Düren, and F.J. Keil, *Study of molecular shape and non-ideality effects on mixture adsorption isotherms of small molecules in carbon nanotubes: A grand canonical Monte Carlo simulation study*, Chem. Eng. Sci. 57 (2002), pp. 2439–2448.
[23] M. Schenk, S.L. Vidal, T.J.H. Vlugt, B. Smit, and R. Krishna, *Separation of alkane isomers by exploiting entropy effects during adsorption on silicalite-1: A configurational-bias Monte Carlo simulation study*, Langmuir 17 (2001), pp. 1558–1570.
[24] S. Jakobtorweihen, N. Hansen, and F.J. Keil, *Molecular simulation of alkene adsorption in zeolites*, Mol. Phys. 103 (2005), pp. 471–489.
[25] H. Rafii-Tabar, *Computational Physics of Carbon Nanotubes*, Cambridge University Press, Cambridge, 2008.
[26] M.G. Martin and J.I. Siepmann, *Transferable potentials for phase equilibria 1. United-atom description of* n-*alkanes*, J. Phys. Chem. B 102 (1998), pp. 2569–2577.
[27] C.D. Wick, M.G. Martin, and J.I. Siepmann, *Transferable potentials for phase equilibria 4. United-atom description of linear and branched alkenes and alkylbenzenes*, J. Phys. Chem. B 104 (2000), pp. 8008–8016.
[28] W.A. Steele, *The Interaction of Gases with Solid Surfaces*, Pergamon, Oxford, 1974.
[29] D. Frenkel and B. Smit, *Understanding Molecular Simulations, from Algorithms to Applications*, 2nd ed., Academic Press, San Diego, 2002.
[30] M.D. Macedonia and E.J. Maginn, *A biased grand canonical Monte Carlo method for simulating adsorption using all-atom and branched united atom models*, Mol. Phys. 96 (1999), pp. 1375–1390.
[31] R. Saito, M. Fujita, G. Dresselhaus, and M.S. Dresselhaus, *Electronic structure of chiral graphene tubules*, Appl. Phys. Lett. 60 (1992), pp. 2204–2206.
[32] T.J.H. Vlugt and M. Schenk, *Influence of framework flexibility on the adsorption properties of hydrocarbons in the zeolite silicalite*, J. Phys. Chem. B 106 (2002), pp. 12757–12763.
[33] S. Jakobtorweihen, M.G. Verbeek, C.P. Lowe, F.J. Keil, and B. Smit, *Understanding the loading dependence of self-diffusion in carbon nanotubes*, Phys. Rev. Lett. 95 (2005), 044501.

[34] M. Allen and D.J. Tildesley, *Computer Simulation of Liquids*, Clarendon Press, Oxford, 1987.

[35] J.I. Siepmann and D. Frenkel, *Configurational bias monte carlo: A new sampling scheme for flexible chains*, Mol. Phys. 75 (1992), pp. 59–70.

[36] D. Frenkel, G. Mooij, and B. Smit, *Novel scheme to study structural and thermal properties of continuously deformable molecules*, J. Phys. Condens Matter 4 (1992), pp. 3053–3076.

[37] S. Jakobtorweihen, N. Hansen, and F.J. Keil, *Combining reactive and configurational-bias Monte Carlo: Confinement influence on the propene metathesis reaction system in various zeolites*, J. Chem. Phys. 125 (2006), 224709.

[38] B.E. Poling, J.M. Prausnitz, and J. O'Connell, *The Properties of Gases and Liquids*, 5th ed., McGraw-Hill, New York, 2000.

[39] B. Smit and J.I. Siepmann, *Computer simulations of the energetics and sitting of* n*-alkanes in zeolites*, J. Phys. Chem. 98 (1994), pp. 8442–8452.

[40] J.F. Denayer, W. Souverijns, A. Jacobs, J.A. Martens, and G.V. Baron, *High-temperature low-pressure adsorption of branched C_5–C_8 alkanes on zeolite beta, zsm-5, zsm-22, zeolite y, and mordenite*, J. Phys. Chem. B 102 (1998), pp. 4588–4597.

[41] B. Smit and J.I. Siepmann, *Simulating the adsorption of alkanes in zeolites*, Science 264 (1994), pp. 1118–1120.

[42] H. Thamm, H. Stach, and G.I. Berezin, *Anfangsadsorptionswärmen von Gasen und Dämpfen an den SiO_2-Molekularsieben US-Ex und Silicalit*, Z. Chem. 24 (1984), pp. 420–421.

[43] C.D. Bruce, T.R. Rybolt, H.E. Thomas, T.E. Agnew, and B.S. Davis, *Two-surface virial analysis of alkane adsorption on carbopack c with and without hydrogen treatment*, J. Colloid Interface Sci. 194 (1997), pp. 448–454.

[44] A.L. Myers and J.M. Prausnitz, *Thermodynamics of mixed gas adsorption*, AIChE J. 11 (1965), pp. 121–127.

[45] J.-C. Charlier, X. Gonze, and J. Michenaud, *First-principles study of carbon nanotube solid-state packings*, Europhys. Lett. 29 (1995), pp. 43–48.

[46] J.K. Holt, H.G. Park, Y. wang, M. Stadermann, A.B. Artyukhin, C. Grigoropoulos, A. Noy, and O. bakajin, *Fast mass transport through sub-2-nanometer carbon nanotubes*, Science 312 (2006), pp. 1034–1037.

[47] B.J. Hinds, N. Chopra, T. Rantell, R. Andrews, V. Gavalas, and L.G. Bachas, *Aligned multiwalled carbon nanotube membranes*, Science 303 (2004), pp. 62–65.

[48] S. Agnihotri and F.-L. Yun, *Fundamental structural properties of single-walled carbon nanotubes: Reopening the debate over hydrogen storage, AIChE Spring National Meeting, Conference Proceedings*, Americal Institute of Chemical Engineers, New York, NY, 2006, p. P43844.